(PCT.202) 8030 Electronics Letters
32(1996) 26 September, No. 20, Stevenage, Herts, GB

XP 000637908

Tunable fibre bandpass filter based on a linearly chirped fibre Bragg grating for wavelength demultiplexing

M.G. Xu, A.T. Alavie, R. Maaskant and M.M. Ohn

E p·1918-1919-② p·d·26-09-1996

Indexing terms: Gratings in fibres, Optical fibre filters

A novel tunable fibre bandpass filter based on a linearly chirped fibre Bragg grating (LCFBG) has been demonstrated. The transmission peaks in the LCFBG stopband are electronically induced by controlling the strain distribution along the LCFBG using a piezoelectric stack. Transmission peaks with 0.58nm bandwidth and 10.6dB rejection ratio have been achieved with a tuning step of 0.28nm over a range of 10nm.

Introduction: The phase-shifted fibre Bragg grating (FBG) is showing promise as an adaptable high finesse transmission filter or switching element for future dense WDM optical communication systems [1]. To date, two techniques for fabricating phase-shifted FBGS have been reported: the phase-shifted phase mask technique [2] and the UV post-processing method [3]. However, high quality phase masks are very expensive and UV post-processing requires tight control of precision, especially in short gratings, and all have limitations when it is desirable to tune the bandpass peak or to provide a wider bandpass peak and rejection band. In this Letter we present a new, yet simple, method for introducing bandpass peaks inside the stopband of an LCFBG, by controlling the strain distribution along the LCFBG. As a result of this arrangement, not only can the bandpass peak be made tunable, but multi-bandpass peaks can also be opened simultaneously.

Principle: Theoretically it has been shown [1] that the introduction of a $\pi/2$ phase-shift at the centre of a uniform (i.e. unchirped) FBG opens a 100% transmission peak within the stopband. The peak shifts either with the amount of phase-shift at the centre location or with the locations of the $\pi/2$ phase-shift. While in principle a broader stopband for a uniform FBG can be achieved using short structures, it could be difficult in the FBG fabrication. Instead, in our scheme we use an LCFBG to increase the stopband.

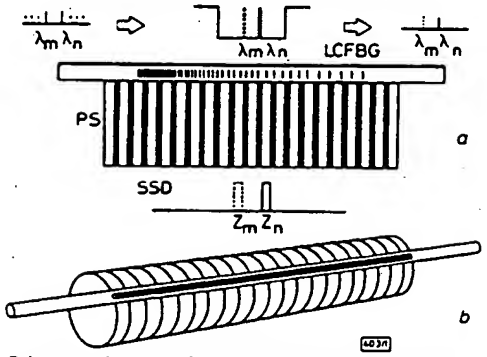

Fig. 1 *Schematic diagram of tunable fibre filter using linearly chirped fibre Bragg grating (LCFBG)*

a Operating principle: bandpass peak varies with location of strain step applied
PS: piezoelectric stack
SSD: strain step distribution
b Perspective view of tunable filter configuration

We assume that an LCFBG with length L can be divided into many grating segments L_n, each of which covers a multiple number of pitches. As an LCFBG reflects different wavelengths at different locations along its length, it satisfies the Bragg condition for a range of wavelengths. Hence when a grating segment is uniformly strained in tension, each wavelength component contributed by the corresponding pitches of that grating segment will be red-shifted, resulting in a transmission peak due to the depletion centred at λ_0. Therefore the peak λ_0 will shift with the location of the grating segment strained, and multiple bandpass peaks within the stopband will occur when multiple segments are strained simultaneously. The magnitude and spectral width of this peak depend on the strain level applied, the length of the grating segment, the chirped rate of the LCFBG, and the grating strength kL.

Experiment and discussion: Fig. 1*a* and *b* depict the tunable fibre filter, where an LCFBG was bonded onto the surface of a segmented piezoelectric stack. A 35mm LCFBG with a reflectivity of 99%, FWHM bandwidth of 13nm, and chirp rate of 0.12nm/mm was used. The 45mm long piezoelectric stack consists of 21 active segments (each ~1.4mm in thickness), with an inactive isolation of ~0.56mm between segments. Each segment can be excited independently, allowing quasi-independent strain control of each segment [4]. Some mechanical coupling between the segments takes place due to the rigidity of the bonding agent. The attached grating experiences the imposed strain distribution and its characteristics can therefore be precisely controlled. The transmission spectrum was obtained by scanning a tunable laser (Intun-1500) with a resolution of 0.01nm, and monitoring the transmitted power.

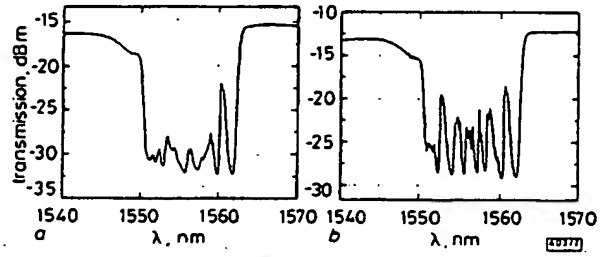

Fig. 2 *High resolution measurement (0.01nm step size) of filter transmission spectral response*

a Single bandpass peak induced with strain step 1/5 distance from one end of LCFBG
b Comb filtering response with multiple strain steps induced at different locations along LCFBG simultaneously

When a single grating segment was strained with a strain step 1/5 of the distance from one end of the LCFBG, a narrow transmission peak opened in the LCFBG stopband, as shown in Fig. 2*a*. In this case, a filter bandwidth of 0.58nm with 10.6dB contrast ratio was achieved. When the location of the strained grating segment was altered, the peak shifted accordingly as predicted (typically 25ms setting time). In fact a tuning step of 0.28nm was achieved, limited by the spatial resolution of the stack. Fig. 2*b* shows a comb filtering response when multiple grating segments were strained simultaneously. This means that by properly controlling the strain distribution, synthesis of various filter responses would also be possible [5]. Another attractive feature is that the number of channels that can be demultiplexed increases with the stopband of the grating. By appropriately designing the LCFBG and piezoelectric stack, the potential demultiplexing capability can be expected to be high. The loss in transmission shown in Fig. 2 was mainly caused by the maximum strain level applied to each grating segment being limited to ~500$\mu\varepsilon$ for the current stack. In addition, owing to the effect of the interaction between the active segments of the piezoelectric stack when strained, the quantitative description of the relative phase change at each grating segment becomes more complicated. A more in-depth analysis of these effects is beyond the scope of this Letter.

Conclusion: We have demonstrated an attractive method for constructing a tunable fibre transmission filter by controlling the strain distribution along an LCFBG using a piezoelectric stack. Multiple bandpass peaks can also be introduced to provide other devices such as comb filters. This offers considerable potential for the WDM applications as a real-time channel filtering/switching element. Work is being directed towards improving the tuning steps and the loss in the bandpass peaks, as well as extending the tunable range.

12 August 1996
Electronics Letters Online No: 19961242

M.G. Xu, A.T. Alavie, R. Maaskant and M.M. Ohn (*ElectroPhotonics Corporation, 7941 Jane Street, Concord, Ontario, L4K 4L6, Canada*)

References

1 AGRAWAL G.P., and RADIC, S.: 'Phase-shifted fibre Bragg gratings and their applications for wavelength demultiplexing', *IEEE Photonics Technol. Lett.*, 1994, 6, (8), pp. 995–997
2 KASHYAP R., MCKEE, P.F., and ARMES, D.: 'UV written reflection grating structures in photosensitive optical fibres using phase-shifted phase masks', *Electron. Lett.*, 1994, 30, (23), pp. 1977–1978
3 CANNING, J., and SCEATS, M.G.: 'π-phase-shifted periodic distributed structures in optical fibres by UV post-processing', *Electron. Lett.*, 1994, 30, (16), pp. 1344–1345
4 ALAVIE, A.T.: 'Method and apparatus of Bragg intra-grating strain control', US patent, 1994
5 ALAVIE, A.T., OHN, M.M., and MAASKANT, R.: 'A tunable Bragg grating device for filter synthesis', Int. Conf. Applications of Photonic Technology, Montreal, Canada, July 1996

Ag^+-Na^+ exchanged waveguides from molten salts in a chemically durable phosphate glass

L.C. Barbosa, N. Aranha, O.L. Alves and R. Srivastava

Indexing terms: Ion exchange, Optical waveguides, Waveguide lasers

The authors report that Ag^+-Na^+ ion exchange has been performed for the first time from molten salt baths in a chemically durable phosphate glass. Characterisation of planar waveguides, fabricated at different temperatures, diffusion times and with varying melt concentrations, indicates large diffusion coefficients and higher index changes with no deterioration of surface quality.

Introduction: Ion exchanged glass waveguides play an important role as passive devices in optical communications [1] and sensors [2], and as active devices in all optical switching [3] and waveguide lasers [4]. In fact, the best figure of merit for nonlinear optical switching requires Kerr-type nonlinearity available in large refractive index glasses [5]. On the other hand, compared to silicate glasses, phosphate glasses are better suited for rare-earth doped glass laser media because of their favourable thermal and spectroscopic properties, even at higher rare-earth ion concentrations [6].

There have been several reports of fabrication of waveguides in rare-earth doped phosphate glasses. The first such report [4] deals with a dry diffusion process where an electric field assisted ion-exchange from a silver stripe was performed in a commercial Nd^{3+}-doped phophate glass (Hoya, LHG-5). The dry process was preferred because most phosphate glasses are known to be prone to chemical attack by molten salts. Recently, interest has shifted towards special compositions of phosphate glasses for ion exchange from molten salts [7, 8]. In [7], K^+-Na^+ exchanged channel waveguides were fabricated from a KNO_3 melt. No information however was given regarding the diffusion rate, index increase, etc. Moreover, it was reported that the process caused a 0.8μm deep depression in the exchanged region of the glass surface, which is an obvious cause of scattering losses. In [8], two-step ion exchange was used in a special glass but no details about the ion pair or exchange process parameters were given. Finally, Ag^+-Na^+ exchange from molten salts in phosphate glasses has not yet been reported.

Recently, the synthesis of a new phosphate glass with much better chemical durability was reported [9, 10]. The glass consists of a mixture of oxides of phosphorus, niobium, lead and sodium. Niobium was added for chemical durability and lead was used to increase the linear refractive index (n = 1.775). The glass fabrication details along with the chemical durability and optical characterisation studies are reported elsewhere [9, 10]. The glass has a transition temperature of Tg 570°C and shows high solubility for rare-earth ions. We have been able to dope this glass with up to 2% by weight of Er_2O_3 without any difficulty. In this Letter, we report the fabrication of waveguides using this phosphate glass, along with a detailed study of the dependence of the waveguide parameters on processing.

Experiment: Planar waveguides were fabricated by immersing polished glass substrates, typically 20mm × 10mm × 1mm in dimensions, in a molten salt bath of equal molar fractions of $NaNO_3$ and KNO_3. This mixture allows ion exchange at temperatures as low as 250°C. The molar fraction of $AgNO_3$ was varied from 0.1 to 5%. The salt was contained in a silica crucible held in a vertical furnace, in which the temperature was controlled to within ±1°C. The sample holder, also made of silica, was attached to a motorised system via a shaft which gradually lowered the sample holder into the salt bath. Ion exchange was performed at three temperatures: 255, 305 and 355°C; and exchange times were 30, 60 and 90 min, respectively. In each case, at least three guided modes were observed in the prism coupler at the wavelength of 632.8nm. This was adequate for determination of the index profile using the InWKB method [11]. No attempt was made to fit the mode index data to any analytical function for the index profile. The surface index change (Δn) and the effective profile depth (d) were estimated as follows:

Δn = difference in the mode-index of the fundamental mode and the substrate index

d = the depth where the index increase reduces to lie of its value at the surface.

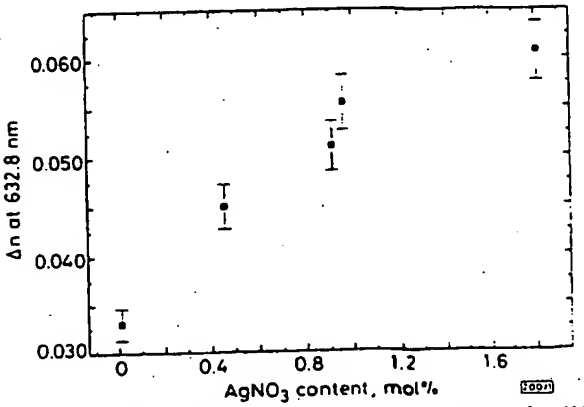

Fig. 1 *Surface index change against the molar concentration of $AgNO_3$ in melt at 355°C*

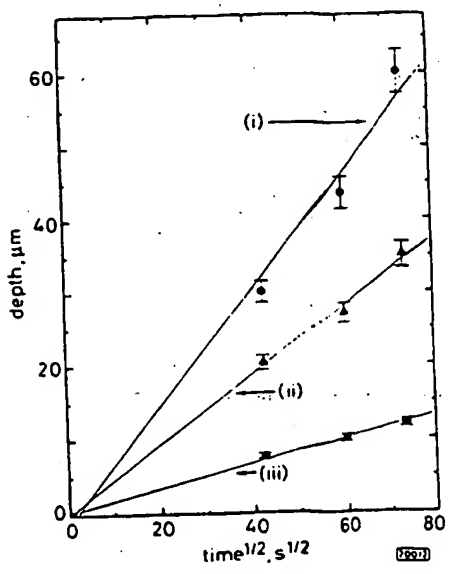

Fig. 2 *Waveguide depth against square-root of time*

For molten bath with 0.5 mol% of $AgNO_3$ content
Effective diffusion coefficients are also shown
(i) $D = 6.19 \times 10^{-13} m^2/s$
(ii) 2.19×10^{-13}
(iii) 3.06×10^{-14}
■ 255°C
▲ 305°C
● 355°C